applied sciences

MDPI

Article

Improved Least Squares Phase Unwrapping Method Based on Chebyshev Filter

Guoqing Li [1], Yake Li [2,*] and Wenyan Liu [3]

[1] College of Mechanical Electrical Engineering, Fujian Agriculture and Forestry University, Fuzhou 350100, China; lgli@fafu.edu.cn
[2] Quanzhou Institute of Equipment Manufacturing Haixi Institute, Chinese Academy of Sciences, Quanzhou 362200, China
[3] College of Computer and Cyber Security, Fujian Normal University, Fuzhou 350117, China; qsz20221402@student.fjnu.edu.cn
* Correspondence: liyake@fjirsm.ac.cn; Tel.: +86-135-9975-1683

Abstract: Phase unwrapping of high phase noise and steep phase gradient has always been a challenging problem in interferometric synthetic aperture radar (InSAR), in which case the least squares (LS) phase unwrapping method often suffers from significant unwrapping errors. Therefore, this paper proposes an improved LS phase unwrapping method based on the Chebyshev filter, which solves the problem of incomplete unwrapping and errors under high phase noise and steep phase gradient. Firstly, the steep gradient phase is transformed into multiple flat gradient phases using the Chebyshev filter. Then the flat gradient phases are unwrapped using the LS unwrapping method. Finally, the final unwrapped phase is obtained by iteratively adding the unwrapping results of the flat gradient phases. The simulation results show that the proposed method has the best accuracy and stability compared to LS, PCUA, and RPUA. In the real InSAR phase unwrapping experiment, the RMSE of the proposed method is reduced by 63.91%, 35.38%, and 54.39% compared to LS, PCUA, and RPUA. The phase unwrapping time is reduced by 62.86% and 11.64% compared to PCUA and RPUA.

Keywords: least squares; phase gradient; phase unwrapping; Chebyshev filter

Citation: Li, G.; Li, Y.; Liu, W. Improved Least Squares Phase Unwrapping Method Based on Chebyshev Filter. *Appl. Sci.* **2024**, *14*, 4894. https://doi.org/10.3390/app14114894

Academic Editors: Roberto Scarpa and Atsushi Mase

Received: 30 April 2024
Revised: 23 May 2024
Accepted: 4 June 2024
Published: 5 June 2024

1. Introduction

Interferometric synthetic aperture radar (InSAR) is a remote sensing technique that combines electromagnetic wave interferometry with synthetic aperture radar (SAR) and extracts information on ground elevation or surface deformation, facilitating ground surveillance and measurement, by processing SAR image data through interferometry [1,2]. In recent years, with the rapid advancement of remote sensing technology and the widespread use of high-resolution satellites, spaceborne InSAR has increasingly become crucial in applications such as ground elevation measurement, surface deformation studies, and atmospheric research [3–6]. InSAR has many advantages in terrain mapping and surface deformation monitoring, such as being robust to time and weather, but the InSAR processing process can be affected by many factors, such as interference decorrelation, atmospheric phase, and phase unwrapping. These factors could cause reduced measurement accuracy or measurement failure, especially for single-baseline InSAR systems.

Among these factors, phase unwrapping is one of the key steps to obtaining high-precision terrain and surface deformation using InSAR [7–9]. The phase unwrapping method used in InSAR processing is directly related to the accuracy of the solved terrain and surface deformation information [10,11]. There still does not exist a suitable phase unwrapping method for all cases, as especially in the case of large phase noise and steep terrain, many phase unwrapping methods will produce large errors. So far, many phase unwrapping methods have been proposed, which can mainly be divided into the following three categories, path-following methods [12–14], optimal estimation methods [15], and

minimum norm methods [16–19], as well as other methods [20–25], such as the Kalman filtering methods [20] and machine learning methods [21,22].

The first category, path-following methods, is represented by the Goldstein branch-cutting method [12,14] and the quality map guidance method [13]. The Goldstein branch-cutting method identifies positive and negative residual points, connects the residual points according to the nearest neighbor principle, and generates "branch cuts". It prevents the propagation of errors by following the principle that the integral path does not cross the "branch cuts". The Goldstein branch-cutting method has the obvious advantages of fast speed and high accuracy under the condition of high signal-to-noise ratio (SNR) and low phase gradient. However, when the noise is large and the phase gradient is steep, it is difficult for this method to accurately connect branch tangents, which often leads to errors in integration path selection and introduces errors into the unwrapping stage [14]. The quality map guidance method does not identify residual points and does not set branch tangents. It is a method that defines the wrapping phase quality through the phase quality map, controls the integration path to advance along the high-quality pixels to the low-quality pixels, and sequentially unwraps the wrapping phase. However, its accuracy depends largely on the reliability of the quality map; when the noise is large and the phase gradient is steep, the residuals will be distributed in the high-quality area, and the quality-map guidance method will not work properly [13].

The second category, optimal estimation methods, such as the network flow method, is also commonly used for phase unwrapping. Unlike the methods mentioned earlier, the network flow method transforms the phase problem into a network flow problem with the concept of minimum cost flow, and it limits the phase error transmission in the low-mass region and obtains a globally optimal solution by minimizing the difference between the phase gradient of the unwrapped phase and the discrete partial derivatives of the unwrapped phase. However, for low SNR and steep phase gradient, the error can still be significant.

Compared to the methods mentioned above, the third category, the minimum norm-based methods, has the fastest unwrapping speed and smoothest phase unwrapping results [15]. The least squares (LS) phase unwrapping method is one of the most commonly used methods of the minimum norm-based methods. The LS phase unwrapping method can be understood as finding the solution to the Poisson equation under Neumann boundary conditions, which can be achieved through iterative methods, discrete cosine transforms (DCT), fast Fourier transform (FFT), and an unweighted multi-level grid method, but it also produces significant unwrapping errors with large phase noise and high phase gradient [17]. In recent years, some scholars have improved the LS phase unwrapping method based on its rapidity and smoothness, making the LS phase unwrapping method suitable for high phase noise and high phase gradient. For example, Xia et al. [26] proposed a phase calibration unwrapping algorithm for phase data corrupted by strong decorrelation speckle noise (PCUA). This algorithm uses the average phase gradient to replace the phase gradient that is greater than the standard deviation when solving the Poisson equation. The advantages of the LS phase unwrapping method can be exploited by reducing the phase gradient, and then the error phase is corrected by the iterative method. However, the phase unwrapping effect is unstable when the phase noise and phase gradient change. After this, to make the phase unwrapping results more stable, Zong et al. [27] proposed a robust phase unwrapping algorithm for noisy and segmented phase measurements (RPUA). When solving the Poisson equation, it uses the sine function to correct the phase gradient, which further improves the phase unwrapping accuracy under high noise and high phase gradient. However, in true interference data phase unwrapping, the results obtained are also unstable.

Based on the above analysis, there are certain difficulties in phase unwrapping. Using traditional category I and category II methods, phase unwrapping under high phase noise and steep phase gradient will produce large errors [24,25]. Xia et al. and Zong et al. show that using iterative LS phase unwrapping can reduce the phase unwrapping error under high phase noise and steep phase gradient, but when calculating the equivalent phase gradient, it is too dependent on the overall steepness of the phase gradient to change the steep phase gradient into a sufficiently large number of flat phase gradients. However, the calculation of an equivalent flat phase gradient is too dependent on the overall steepness of the phase gradient. It is difficult to change a steep phase gradient into a sufficiently flat phase gradient.

Therefore, to make the LS phase unwrapping method more stable under high phase noise and high phase gradient, this paper proposes an improved LS phase unwrapping method based on the Chebyshev filter [28] and designs its adaptive filtering threshold so that the high phase gradient is changed into flatter phase gradient as much as possible. Finally, an iterative method of unwrapping phase errors is used to eliminate errors under high phase noise and steep phase gradient.

This paper is organized as follows: Section 2 describes the principle of LS phase unwrapping and the improvement method of this paper. Section 3 is the experimental results and analysis part. Section 4 is a discussion of phase unwrapping methods. Section 5 is the conclusion of this paper.

2. Methods

2.1. The Least Squares Phase Unwrapping Method

In InSAR processing, the wrapped phase is the principal value of the original absolute phase, wrapping between $-\pi$ and π [10]. Phase unwrapping is the process of recovering the original phase from the wrapped phase. The phase obtained by phase unwrapping is called the unwrapped phase. The LS phase unwrapping method treats phase unwrapping as an optimization problem, specifically, finding the minimum value of the unwrapped phase and the wrapped phase gradient. Mathematically, it can be represented as follows [16]:

$$Min = \sum_{i=0}^{M-2}\sum_{j=0}^{N-1}\left|\phi_{i+1,j} - \phi_{i,j} - \Delta_{i,j}^{x}\right|^2 + \sum_{i=0}^{M-1}\sum_{j=0}^{N-2}\left|\phi_{i,j+1} - \phi_{i,j} - \Delta_{i,j}^{y}\right|^2, \tag{1}$$

where M, N represent the horizontal and vertical size of the phase matrix, $\phi_{i,j}$ represents the unwrapped phase, and $\Delta_{i,j}^{x}, \Delta_{i,j}^{y}$ represent the horizontal phase gradient and vertical phase gradient, respectively. The progress can be expressed as follows [16]:

$$\begin{array}{c} \Delta_{i,j}^{x} = W\left(\varphi_{i+1,j} - \varphi_{i,j}\right) \ (i = 0, 1 \ldots M-2; j = 0, 1 \ldots, N-1) \\ \Delta_{i,j}^{x} = 0 \qquad\qquad otherwise \\ \Delta_{i,j}^{y} = W\left(\varphi_{i,j+1} - \varphi_{i,j}\right) \ (i = 0, 1 \ldots M-1; j = 0, 1 \ldots, N-2) \\ \Delta_{i,j}^{y} = 0 \qquad\qquad otherwise, \end{array} \tag{2}$$

where W represents the wrapped symbol, and $\varphi_{i,j}$ represents the wrapped phase.

From Equation (1), we can derive the following [16]:

$$\left(\phi_{i+1,j} - 2\phi_{i,j} + \phi_{i-1,j}\right) + \left(\phi_{i,j+1} - 2\phi_{i,j} + \phi_{i,j-1}\right) = \rho_{i,j}, \tag{3}$$

where [16]

$$\rho_{i,j} = \Delta_{i,j}^{x} - \Delta_{i-1,j}^{x} + \Delta_{i,j}^{y} - \Delta_{i,j-1}^{y}. \tag{4}$$

We can obtain the unwrapped phase by using discrete cosine transform [16]:

$$\phi_{i,j} = DCT^{-1}\left\{\frac{DCT\{\rho_{i,j}\}}{2\left(\cos\left(\pi\frac{i}{M}\right)+cos\left(\pi\frac{j}{N}\right)-2\right)}\right\}, \quad (5)$$

where DCT and DCT^{-1}, respectively, represent discrete cosine transform and discrete inverse cosine transform [16].

2.2. The Improved Least Squares Phase Unwrapping Method

Assuming there are no phase discontinuities in the wrapped phase, the unwrapped phase is accurate. However, when noise and steep phase gradient are present, there will be phase discontinuities in the wrapped phase [27]. Therefore, the phase gradient exists:

$$\Delta\phi_{i,j} \neq \Delta\varphi_{i,j}, \quad (6)$$

where $\Delta\phi_{i,j}$ represents the gradient of the unwrapped phase, and $\Delta\varphi_{i,j}$ represents the gradient of the wrapped phase; thus, there must inevitably exist

$$\delta_{i,j} = W(\phi_{i,j} - \varphi_{i,j}), \quad (7)$$

where $\delta_{i,j}$ represents the errors of the unwrapped phase.

Using the LS phase unwrapping method in this case does not generate good results. In other words, when there are multiple phase discontinuities, the LS phase unwrapping method will produce larger errors [26,27]. Considering that the LS phase unwrapping method has a fast and continuous phase unwrapping effect under low noise and flat phase and that it is equivalent to multiple low flat phase maps using the LS phase unwrapping method for phase unwrapping under high noise and steep phase gradient, it can be expressed that

$$\varphi_{i,j} = W(\phi_{i,j}) = W\left(\sum_{k=1}^{N}\phi_{i,j}^{k}\right) \quad (8)$$

However, how to equalize the low phase gradient and how to determine the number of low phase gradients is a difficult problem. To solve this problem, we think of the phase gradient as a form of a discrete signal, employing a Chebyshev low-pass filter to filter the phase gradient, and use an iterative method to determine the number of low phase gradients.

The Chebyshev low-pass filter has a steep transition band, which can effectively change the steep phase gradient into a flat phase gradient for the stopband phase gradient. In addition, to preserve the phase characteristics, the passband phase gradient is not filtered. When the type I second-order Chebyshev filter is improved and applied to phase gradient filtering, the transfer function can be represented as follows [28]:

$$H(\Delta_{i,j}) = \begin{cases} \sqrt{\frac{1}{1+\varepsilon^2 T_2^2\left(\frac{\Delta_{i,j}}{\Delta_c}\right)}} & \left(|\Delta_{i,j}| > \Delta_c\right) \\ \Delta_{i,j}^{\delta} & \left(|\Delta_{i,j}| \leq \Delta_c\right), \end{cases} \quad (9)$$

where $\Delta_{i,j}$ represents the unwrapped phase gradient of x or y direction, which is $\Delta_{i,j}^{x}$ or $\Delta_{i,j}^{y}$, and ε represents the fluctuation coefficient of the ripple magnitude within the passband. We set the maximum allowable attenuation in the passband to be 1 dB; it is about 0.707. Δ_c represents the cut-off phase of the passband, which is set to the standard deviation of

the phase gradient, and $T_2(\dots)$ represents the second-order Chebyshev polynomial. These formulas can be expressed as follows:

$$\begin{gathered} \frac{1}{1+\varepsilon^2} \approx 0.707 \\ \Delta_c = \sqrt{\frac{\sum_{i=1}^{M}\left(\Delta_{i,j}-\mu\right)^2}{M}} \\ \mu = \frac{\sum_{i=1}^{M}\Delta_{i,j}}{M} \\ T_2(\dots) = \cosh(2arccosh(\dots)), \end{gathered} \tag{10}$$

where $1/\left(1+\varepsilon^2\right)$ represents the maximum allowable attenuation in the passband, *cosh* and *arccosh* represent hyperbolic cosine and inverse hyperbolic cosine functions, and in the direction of j is the same equation.

Secondly, the filtered phase gradient is used for phase unwrapping:

$$\phi_{i,j}^{k} = DCT^{-1}\left\{\frac{DCT\left\{\rho_{i,j}^{k}\right\}}{2\left(\cos\left(\pi\frac{i}{M}\right)+cos\left(\pi\frac{j}{N}\right)-2\right)}\right\}, \tag{11}$$

where

$$\rho_{i,j}^{k} = H\left(\Delta_{i,j}^{x}\right) - H\left(\Delta_{i-1,j}^{x}\right) + H\left(\Delta_{i,j}^{y}\right) - H\left(\Delta_{i,j-1}^{y}\right). \tag{12}$$

By Equation (8), if there is the incomplete unwrapped phase, there must inevitably exist $\phi_{i,j}^{k+1}$:

$$\phi_{i,j}^{k+1} = DCT^{-1}\left\{\frac{DCT\left\{\rho_{i,j}^{k+1}\right\}}{2\left(\cos\left(\pi\frac{i}{M}\right)+cos\left(\pi\frac{j}{N}\right)-2\right)}\right\}, \tag{13}$$

$$\rho_{i,j}^{k+1} = H\left(\Delta\delta_{i,j}^{x}\right) - H\left(\Delta\delta_{i-1,j}^{x}\right) + H\left(\Delta\delta_{i,j}^{y}\right) - H\left(\Delta\delta_{i,j-1}^{y}\right), \tag{14}$$

where $\Delta\delta_{i,j}^{x}$ represents the error phase gradient.

Then, if

$$Avg\left|\phi_{i,j}^{k+1} - \phi_{i,j}^{k}\right| > e \; or \; N > Nit, \tag{15}$$

the wrapped phase can be regarded as fully unwrapping, where *Avg* represents the mean-finding operation, and $|\cdots|$ represents the absolute value operation. e is a very small number, and this paper sets it to 10^{-3}; in this case, it can be considered as completely unwrapping. Nit represents the maximum number of iterations, and this paper sets it to 300, preventing the unwrapping process from not converging.

Finally, the unwrapped phase can be obtained as follows:

$$\phi_{i,j} = \sum_{k=1}^{N}\phi_{i,j}^{k}. \tag{16}$$

The proposed method is represented by the block diagram in Figure 1, which consists of the following main steps:

1. Calculated phase gradient;
2. The parameters of the Chebyshev filter are determined according to the phase gradient;
3. The Chebyshev filter is used for phase gradient filtering;
4. Iteratively recover the entire wrapped phase.

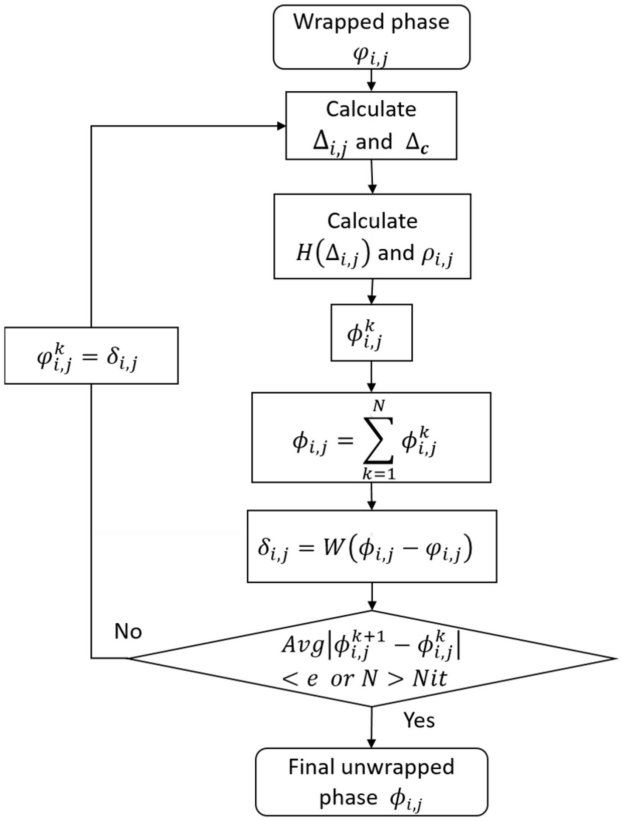

Figure 1. Flow chart of the proposed method.

3. Results

The simulated data and the real InSAR phase data are used in this section to verify the effectiveness of the proposed method of unwrapping. The simulated wrapped phase data were generated using the PEAKS function in MATLAB (Version 9.8.0.1323502, R2020a), and the real InSAR phase data were obtained by InSAR processing of the Sentinel-1 satellite [29].

To verify the superiority of the improved LS phase unwrapping method in this paper, we compared the proposed method with traditional LS, as well as the recently improved LS phase unwrapping methods, PCUA and RPUA. The proposed method is an improvement on the LS method, so the LS method was used in the comparison. PCUA and RPUA are also improved methods of the LS method in recent years and have good phase unwrapping effects. Therefore, comparison with LS, PCUA, and RPUA can better demonstrate the effectiveness of our proposed method.

The iterative method is also used in PCUA and RPUA, and $e = 10^{-3}$ and $Nit = 300$ are set in the experiment. Root mean square error (RMSE) between the unwrapped phase and the true phase is used to evaluate the quality of phase unwrapping [30]:

$$RMSE = \sqrt{\frac{1}{M \times N} \sum_{i=1}^{M} \sum_{j=1}^{N} (\phi_{i,j} - \varphi_{i,j})^2}. \quad (17)$$

3.1. The Simulated Data Results

The simulated wrapped phase was generated using the PEAKS function in MATLAB with a peak to valley of 10, with an adding Gaussian noise of 0 mean and 1 standard deviation. The simulated data have a horizontal and vertical size of 512 × 512, as shown in Figure 2. The color bar on the right side of the figures represents the phase value, the unit is rad.

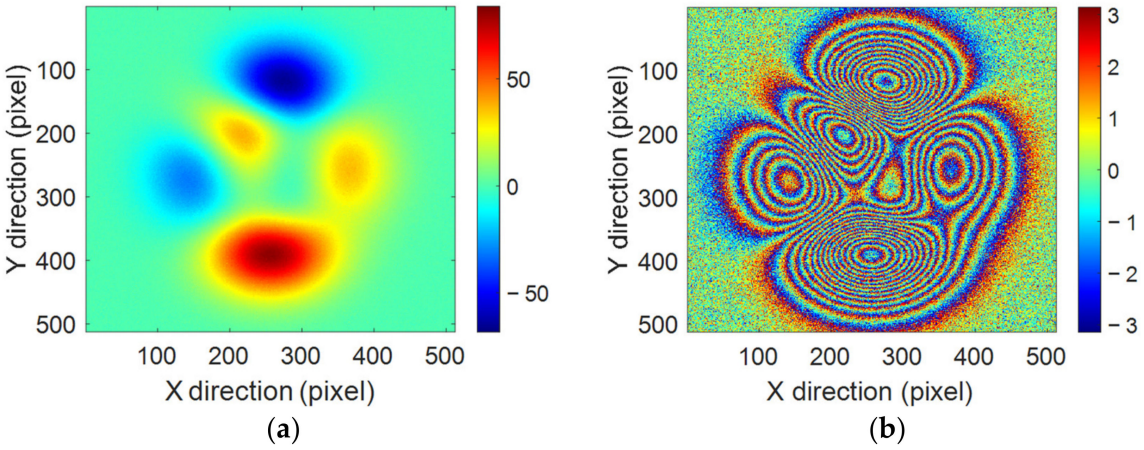

Figure 2. The simulated original phase and wrapped phase. (**a**) The simulated original phase. (**b**) The wrapped phase.

In Figure 2a, the highest phase is 83.84 rad and the lowest phase is −68.23 rad. The wrapped phase map is shown in Figure 2b. Since the wrapped phase is distributed between $-\pi$ and π, noise with a standard deviation of 1 is added, which satisfies the high-noise situation. When the Y direction is at the 250th pixel, the phase gradient map of Figure 2b is shown in Figure 3, which shows that the simulated phase has a steep phase gradient. Therefore, the simulated phase used has a large noise and steep phase gradient, which has a positive effect on verifying the method proposed in this paper.

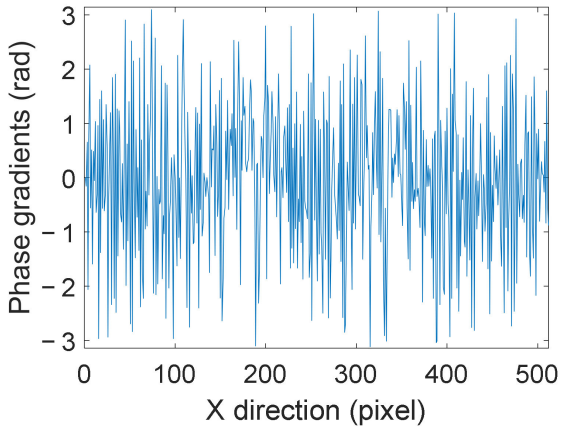

Figure 3. The phase gradient of Figure 2b when the Y direction is at the 250th pixel.

Then, LS, PCUA, RPUA, and the proposed method are used for phase unwrapping. The unwrapping error maps are shown in Figure 4. Table 1 presents the time and RMSE values for each of the four methods. As shown in Figure 4a, the LS phase unwrapping method has a lot of unwrapped areas. As shown in Table 1, the advantage of the LS phase unwrapping method is that it can perform phase unwrapping fastest. But it has the largest RMSE and the worst unwrapping effect. As shown in Figure 4b,c, PCUA and RPUA have greatly improved the LS phase unwrapping method, and have good phase unwrapping results, but there are still a few unwrapped areas. As shown in Table 1, PCUA and RPUA have smaller RMSE compared to the LS phase unwrapping method but require more unwrapping time, which has room for improvement. As shown in Figure 4d, the proposed method has the least unwrapped areas, and as shown in Table 1, the proposed method has the smallest RMSE, which is reduced by 94.53% compared with LS, 31.50% compared with PCUA and 15.11% compared with RPUA. The proposed method has a faster unwrapping speed compared with PCUA and RPUA, which is improved by 55.29%

and 10.91%. Therefore, this simulation experiment shows that the proposed method has a better effect than LS, PCUA, and RPUA.

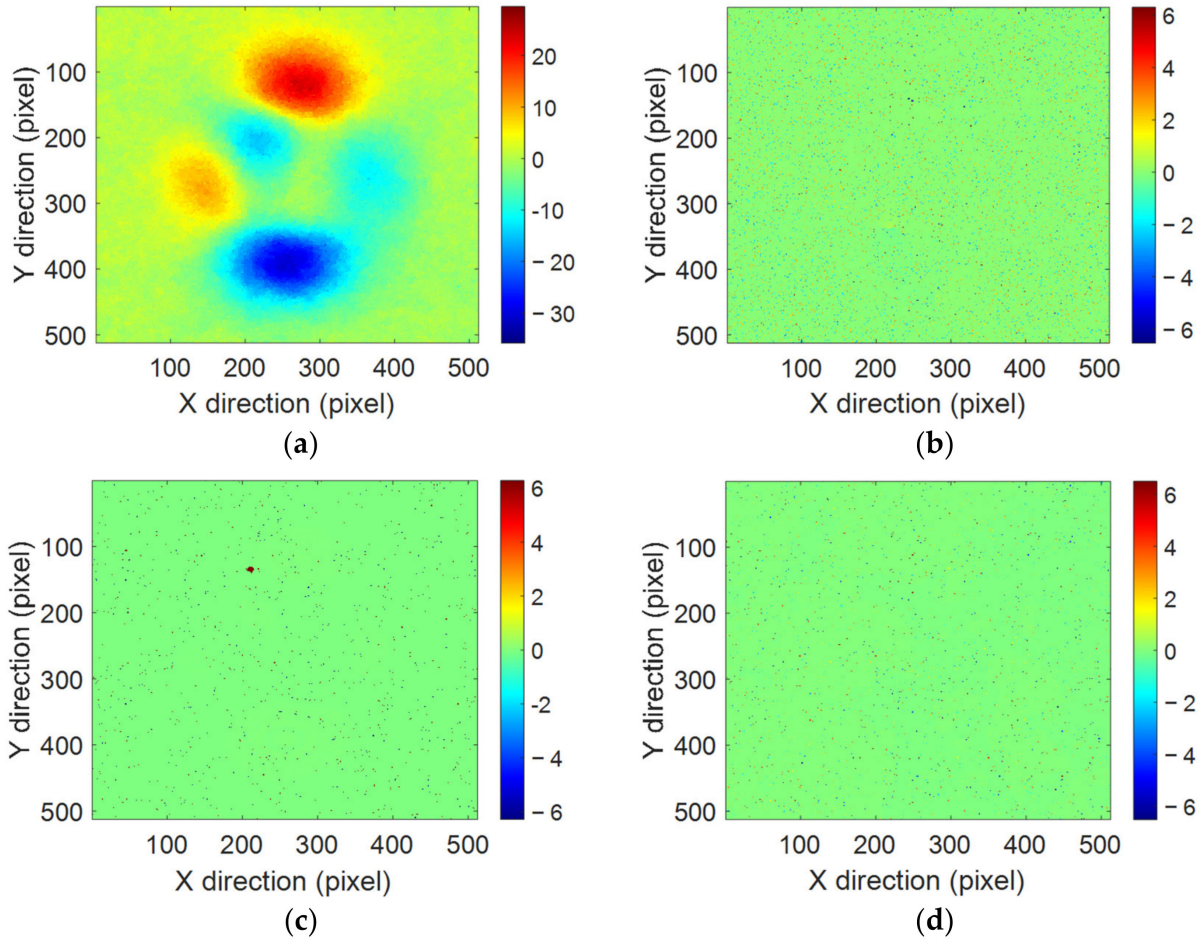

Figure 4. The error maps result from simulated phase unwrapping. (**a**) LS phase unwrapping error map. (**b**) PCUA phase unwrapping error map. (**c**) RPUA phase unwrapping error map. (**d**) The proposed method phase unwrapping error map.

Table 1. The time and RMSE values for each of the four methods.

Methods	Times (s)	RMSE (rad)
LS	0.0468	7.2621
PCUA	5.8232	0.5797
RPUA	2.9227	0.4678
Proposed	2.6037	0.3971

Furthermore, to test the robustness of the proposed method, phase unwrapping tests were performed by increasing the phase gradient while keeping the noise constant. Based on the above simulated experimental data, the same MATLAB PEAKS function was used to generate experimental data. While the noise standard deviation remained unchanged at 1, the peak to the valley gradually increased from 10 to 15. The RMSE of the unwrapping results with different phase gradients is shown in Figure 5. Among them, the RMSE of LS phase unwrapping is the largest and gradually increases as the phase gradient increases. The unwrapping effect is the worst and is not suitable for steep phase unwrapping. PCUA, RPUA, and the proposed method can all achieve lower RMSE than LS and can perform stable phase unwrapping under a high phase gradient compared to LS. However, when the peaks to the valley is 13.5, the RMSE of the unwrapping results of PCUA and RPUA

will mutate and be unstable. For proposed the method, compared with the other three methods, the RMSE of the unwrapping results has always been at the lowest, and there is no RMSE mutation when the phase gradient changes. Therefore, the proposed method is very little affected by the phase gradient can almost be ignored, and can perform stable phase unwrapping at steep phases.

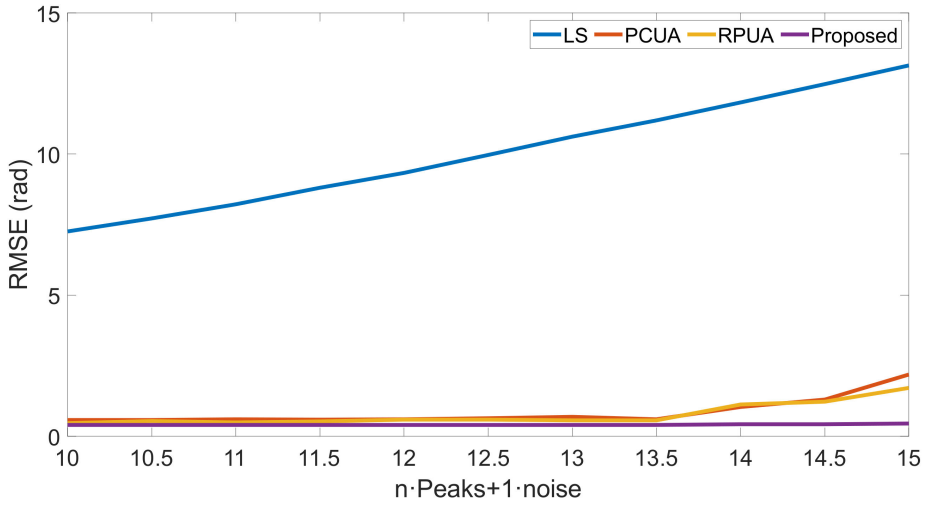

Figure 5. The RMSE with different phase gradients of the four methods.

Then, with the peak to the valley constant at 10, the standard deviation of the noise is gradually increased from 1 to 1.5, and the unwrapped resulting RMSE is shown in Figure 6. Like the above phase unwrapping results, the RMSE of LS phase unwrapping is the largest and gradually increases with the increase in phase noise. The phase unwrapping effect of LS is the worst and is not suitable for phase unwrapping under high noise. PCUA, RPUA, and the proposed method all improve the effect of LS phase unwrapping under the influence of noise. From the RMSE of the phase unwrapping results in Figure 6, it can be seen that RPUA is affected by phase noise the most compared to PCUA and the proposed method. The phase unwrapping results of the proposed method have the lowest RMSE and are least affected by phase noise. Therefore, the proposed method has the best phase unwrapping effect under high noise compared with LS, PCUA, and RPUA.

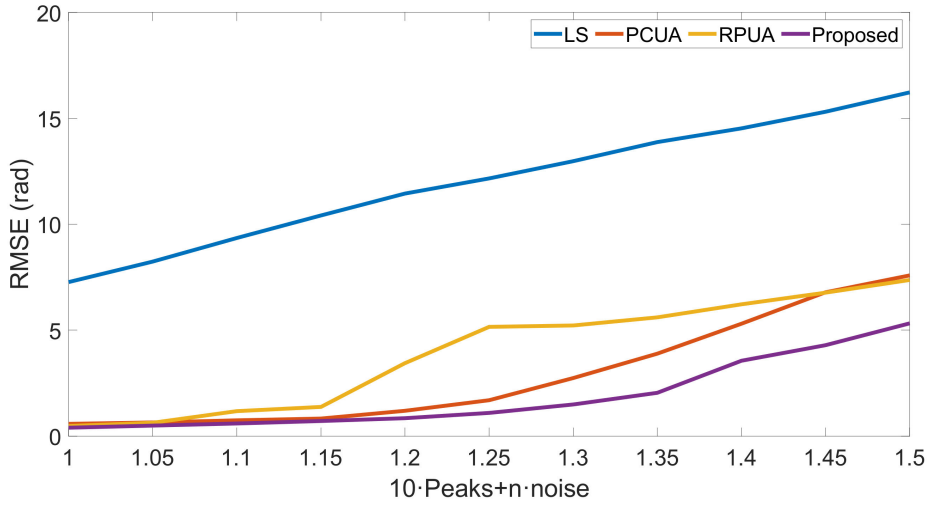

Figure 6. The RMSE with different phase noises of the four methods.

According to the above simulation data analysis, the method proposed in this paper has the best robustness compared with LS, PCUA, and RPUA under different phase gradients and different phase noises.

3.2. The Real InSAR Phase Unwrapping Results of Sentinel-1

We selected two sentinel-1 IW data from 12 January 2023 and 24 January 2023 covering the position (30.43 N, 103.02 E), and the experimental data are distributed over strip 6 of IW2. The Sentinel-1 satellite is a C-band SAR launched by ESA in 2014; its data are currently available for free on the Copernicus Data Space Ecosystem. It has been widely used in marine environment monitoring, land change detection, earthquake detection, and landslide detection. Using real Sentinel-1 InSAR phase data for phase unwrapping experiments can better reflect the advantages and disadvantages of the phase unwrapping algorithm.

The terrain data located in Yaan City, Sichuan Province, China, with a maximum and minimum elevation difference of about 500 m was used. Before phase unwrapping, 1×5 multi-looking was applied to the data in azimuth and range. Phase interference was performed after image registration. Then the reference ellipsoid phase was removed, and then the Goldstein filter [31] with a coefficient of 0.5 was selected for phase filtering, and finally, a 500×500 wrapped phase map in the horizontal and vertical was obtained. As shown in Figure 7a, it can be seen that the phase interference fringes are relatively dense and there is a large amount of noise residue, which provides favorable conditions for verifying the effectiveness of this method. Figure 7b shows the real-terrain simulated phase, which uses the Digital Elevation Model of Shuttle Radar Topography Mission [32] information and was generated under the same conditions as the InSAR phase data.

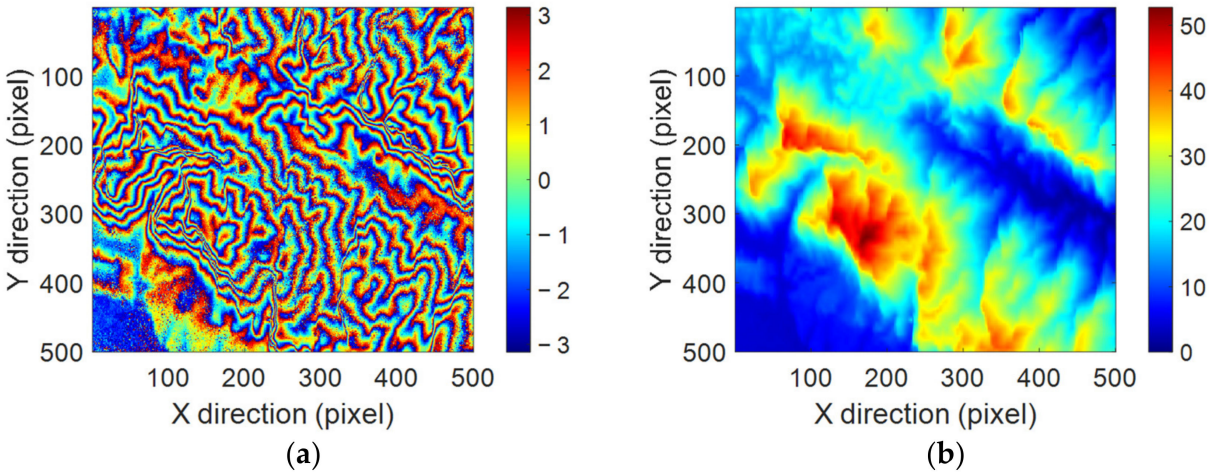

Figure 7. The wrapped phase data and the real phase data. (**a**) The wrapped phase. (**b**) The real phase data.

Using the same unwrapping methods as the simulated test, the unwrapping error results are shown in Figure 8 and Table 2.

Table 2. The times, error range, and RMSE of the true phase unwrapping.

Methods	Times (s)	Error Range (rad)	RMSE (rad)
LS	0.0483	[−13.4945, 10.9733]	4.6728
PCUA	8.1418	[−11.0035, 8.4564]	2.6099
RPUA	3.4221	[−13.5213, 9.5692]	3.6979
Proposed	3.0237	[−9.2915, 6.9055]	1.6866

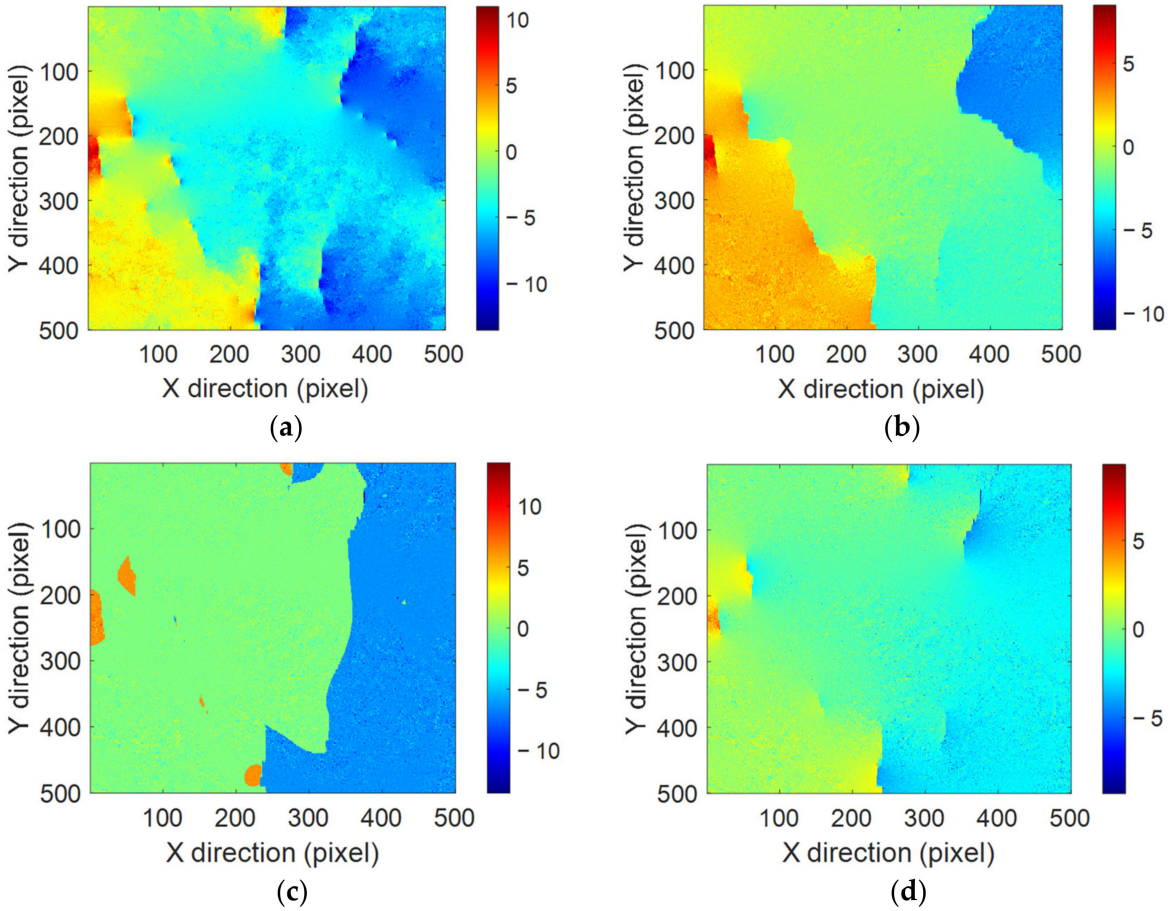

Figure 8. The error maps resulting from true phase unwrapping. (**a**) LS phase unwrapping error map. (**b**) PCUA phase unwrapping error map. (**c**) RPUA phase unwrapping error map. (**d**) The proposed method phase unwrapping error map.

It can be seen from Figure 8a that the incompletely unwrapped phase range in the error map obtained by the LS phase unwrapping method is the highest. From Table 2, it can be seen that the RMSE obtained by the LS phase unwrapping method is the largest and the error range is the widest; its biggest advantage is that it can be quickly unwrapping. It can be seen from Figure 8b,c that PCUA and RPUA reduce the incompletely unwrapped area and phase range compared to the LS phase unwrapping method, but there will still be more incompletely unwrapped areas and larger phase error. As can be seen from Table 2, PCUA takes the most phase unwrapping time but has a lower RMSE than LS and RPUA. Although RPUA reduces the processing time, it has a larger RMSE and a wider error range than PCUA. As can be seen from Figure 8d and Table 2, the proposed method has the smallest incomplete unwrapping area and the smallest incomplete unwrapping phase range, and the unwrapping time is about 62.86% and 11.64% shorter than PCUA and RPUA, respectively. Compared with LS, PCUA, and RPUA, the proposed method has the smallest RMSE, which is reduced by 63.91%, 35.38%, and 54.39%, respectively.

4. Discussion

InSAR has many advantages in terrain height measurement and surface deformation measurement, but InSAR processing will be affected by many factors, especially in terms of phase unwrapping, which will directly affect the accuracy of the measurement results. Currently, existing phase unwrapping methods have certain flaws, and there is currently no perfect phase unwrapping method suitable for all situations. Especially when the phase

noise is large and the phase gradient is steep, the mainstream phase unwrapping methods will produce large unwrapping errors.

In recent years, many researchers have made improvements to the LS phase unwrapping method to make it suitable for high phase noise and steep phase gradient, such as PCUA and RPUA, which are experimentally compared in this paper. However, there will still be a large phase unwrapping error, and when the phase noise and phase gradient change, PCUA and RPUA are unstable, and the generated RMSE is sudden.

Therefore, this paper makes further improvements based on LS phase unwrapping. In experiments, it was found that the factor that affects the accuracy of phase unwrapping is the phase gradient, and noise is also one of the factors that affect the change of the phase gradient. When the phase gradient is relatively flat, the LS phase unwrapping method can perform phase unwrapping quickly and accurately. However, when the phase gradient is steep, the LS phase unwrapping method can only perform phase unwrapping quickly and cannot accurately obtain phase unwrapping results. Therefore, this paper uses a low-pass filter to change the steep phase gradient into a flat phase gradient for phase unwrapping. Based on the properties of many low-pass filters, the Chebyshev low-pass filter is selected and improved, which is added in phase unwrapping. To maintain the phase characteristics, an iterative method is used to add all the phase unwrapped results after low-pass filtering to obtain the final unwrapped phase.

5. Conclusions

This paper proposes an improved least squares phase unwrapping method based on the Chebyshev filter. The accuracy and robustness of the method were verified by comparing the simulated phase and the real InSAR phase. Simulation data indicate that the proposed method's RMSE is 94.53%, 31.50%, and 15.11% lower than that of LS, PCUA, and RPUA, respectively. The proposed method has a faster unwrapping speed compared with PCUA and RPUA, which is improved by 55.29% and 10.91%. The robustness of the proposed method was validated through its performance in phase unwrapping under varying phase gradients and phase noise. Under the real InSAR phase unwrapping, the phase unwrapping RMSE of the proposed method is reduced by 63.91%, 35.38%, and 54.39% compared to LS, PCUA, and RPUA. The phase unwrapping time is reduced by 62.86% and 11.64% compared to PCUA and RPUA. Based on the analysis of the above results, the proposed method has the most accurate unwrapping effect and best robustness compared to LS, PCUA, and RPUA.

However, in the simulated and real phase unwrapping results obtained, there is still some incompletely unwrapped phase, and the proposed method speed is slower than the LS phase unwrapping speed. In the future, the speed and efficiency of the phase unwrapping can be improved by adding more appropriate filters to divide the phase of the steep gradient into more flat gradient phases or adding Chebyshev filters to other phase unwrapping methods to improve the phase unwrapping effect of other methods.

Author Contributions: Conceptualization, G.L.; Methodology, G.L.; Investigation, W.L.; Writing—original draft, G.L.; Writing—review & editing, Y.L.; Project administration, Y.L. All authors have read and agreed to the published version of the manuscript.

Funding: This research received no external funding.

Institutional Review Board Statement: Not applicable.

Informed Consent Statement: Not applicable.

Data Availability Statement: The raw data supporting the conclusions of this article will be made available by the authors on request.

Conflicts of Interest: The authors declare no conflict of interest.

References

1. Pepe, A.; Calò, F. A Review of Interferometric Synthetic Aperture RADAR (InSAR) Multi-Track Approaches for the Retrieval of Earth's Surface Displacements. *Appl. Sci.* **2017**, *7*, 1264. [CrossRef]
2. Chindo, M.M.; Hashim, M.; Rasib, A.W. Challenges of Insar Dem Derivation with Sentinel-1 Sar in Densely Vegetated Humid Tropical Environment. *Int. Arch. Photogramm. Remote Sens. Spat. Inf. Sci* **2023**, *48*, 93–98. [CrossRef]
3. Bernardi, M.S.; Africa, P.C.; De Falco, C.; Formaggia, L.; Menafoglio, A.; Vantini, S. On the Use of Interferometric Synthetic Aperture Radar Data for Monitoring and Forecasting Natural Hazards. *Math. Geosci.* **2021**, *53*, 1781–1812. [CrossRef]
4. Zhu, C.; Wang, C.; Zhang, B.; Qin, X.; Shan, X. Differential Interferometric Synthetic Aperture Radar Data for More Accurate Earthquake Catalogs. *Remote Sens. Environ.* **2021**, *266*, 112690. [CrossRef]
5. Liu, Z.; Zhou, C.; Fu, H.; Zhu, J.; Zuo, T. A Framework for Correcting Ionospheric Artifacts and Atmospheric Effects to Generate High Accuracy InSAR DEM. *Remote Sens.* **2020**, *12*, 318. [CrossRef]
6. Malz, P.; Meier, W.; Casassa, G.; Jaña, R.; Skvarca, P.; Braun, M.H. Elevation and Mass Changes of the Southern Patagonia Icefield Derived from TanDEM-X and SRTM Data. *Remote Sens.* **2018**, *10*, 188. [CrossRef]
7. Wu, Z.; Guo, W.; Lu, L.; Zhang, Q. Generalized Phase Unwrapping Method That Avoids Jump Errors for Fringe Projection Profilometry. *Optics Express* **2021**, *29*, 27181–27192. [CrossRef] [PubMed]
8. Li, S.; Xu, W.; Li, Z. Review of the SBAS InSAR Time-Series Algorithms, Applications, and Challenges. *Geod. Geodyn.* **2022**, *13*, 114–126. [CrossRef]
9. Zhang, Y.; Meng, X.M.; Dijkstra, T.A.; Jordan, C.J.; Chen, G.; Zeng, R.Q.; Novellino, A. Forecasting the Magnitude of Potential Landslides Based on InSAR Techniques. *Remote Sens. Environ.* **2020**, *241*, 111738. [CrossRef]
10. Yu, H.; Lan, Y.; Yuan, Z.; Xu, J.; Lee, H. Phase Unwrapping in InSAR: A Review. *IEEE Geosci. Remote Sens. Mag.* **2019**, *7*, 40–58. [CrossRef]
11. Wang, K.; Kemao, Q.; Di, J.; Zhao, J. Deep Learning Spatial Phase Unwrapping: A Comparative Review. *Adv. Photonics Nexus* **2022**, *1*, 014001. [CrossRef]
12. Goldstein, R.M.; Zebker, H.A.; Werner, C.L. Satellite Radar Interferometry: Two-Dimensional Phase Unwrapping. *Radio Sci.* **1988**, *23*, 713–720. [CrossRef]
13. Zhong, H.; Li, H. Path-Following Phase Unwrapping Algorithm Based on Priority-Guided Map. In Proceedings of the 2021 14th International Congress on Image and Signal Processing, BioMedical Engineering and Informatics (CISP-BMEI), Shanghai, China, 23–25 October 2021.
14. De Souza, J.C.; Oliveira, M.E.; Dos Santos, P.A.M. Branch-Cut Algorithm for Optical Phase Unwrapping. *Opt. Lett.* **2015**, *40*, 3456–3459. [CrossRef] [PubMed]
15. Costantini, M. A Novel Phase Unwrapping Method Based on Network Programming. *IEEE Trans. Geosci. Remote Sens.* **1998**, *36*, 813–821. [CrossRef]
16. Ghiglia, D.C. Two-Dimentional Phase Unwrapping: Theory. *Algorithms Softw.* **1998**. Available online: https://cir.nii.ac.jp/crid/1570854175873375232 (accessed on 29 April 2024).
17. Ghiglia, D.C.; Romero, L.A. Minimum Lp-Norm Two-Dimensional Phase Unwrapping. *JOSA A* **1996**, *13*, 1999–2013. [CrossRef]
18. Guo, Y.; Chen, X.; Zhang, T. Robust Phase Unwrapping Algorithm Based on Least Squares. *Opt. Lasers Eng.* **2014**, *63*, 25–29. [CrossRef]
19. Xu, Z.; Lu, T.; Huang, B. Fast Frequency Estimation Algorithm by Least Squares Phase Unwrapping. *IEEE Signal Process. Lett.* **2016**, *23*, 776–779. [CrossRef]
20. Zhang, Y.; Zhang, S.; Gao, Y.; Li, S.; Jia, Y.; Li, M. Adaptive Square-Root Unscented Kalman Filter Phase Unwrapping with Modified Phase Gradient Estimation. *Remote Sens.* **2022**, *14*, 1229. [CrossRef]
21. Gontarz, M.; Dutta, V.; Kujawińska, M.; Krauze, W. Phase Unwrapping Using Deep Learning in Holographic Tomography. *Opt. Express* **2023**, *31*, 18964–18992. [CrossRef] [PubMed]
22. Chen, J.; Kong, Y.; Zhang, D.; Fu, Y.; Zhuang, S. Two-Dimensional Phase Unwrapping Based on U^2-Net in Complex Noise Environment. *Opt. Express* **2023**, *31*, 29792–29812. [CrossRef] [PubMed]
23. An, H.; Cao, Y.; Li, H.; Zhang, H. Temporal Phase Unwrapping Based on Unequal Phase-Shifting Code. *IEEE Trans. Image Process.* **2023**, *32*, 1432–1441. [CrossRef] [PubMed]
24. Oliver-Cabrera, T.; Jones, C.E.; Yunjun, Z.; Simard, M. InSAR Phase Unwrapping Error Correction for Rapid Repeat Measurements of Water Level Change in Wetlands. *IEEE Trans. Geosci. Remote Sens.* **2021**, *60*, 5215115. [CrossRef]
25. Yue, J.; Huang, Q.; Liu, H.; He, Z.; Zhang, H. Multi-Baseline Phase Unwrapping with a Refined Parametric Pure Integer Programming for Noise Suppression. *IEEE J. Miniaturization Air Space Syst.* **2024**. [CrossRef]
26. Xia, H.; Montresor, S.; Guo, R.; Li, J.; Yan, F.; Cheng, H.; Picart, P. Phase Calibration Unwrapping Algorithm for Phase Data Corrupted by Strong Decorrelation Speckle Noise. *Opt. Express* **2016**, *24*, 28713–28730. [CrossRef] [PubMed]
27. Zong, Y.; Duan, M.; Yu, C.; Li, J. Robust Phase Unwrapping Algorithm for Noisy and Segmented Phase Measurements. *Opt. Express* **2021**, *29*, 24466–24485. [CrossRef]
28. Dell'Accio, F.; Di Tommaso, F.; Nudo, F. Generalizations of the Constrained Mock-Chebyshev Least Squares in Two Variables: Tensor Product vs Total Degree Polynomial Interpolation. *Appl. Math. Lett.* **2022**, *125*, 107732. [CrossRef]
29. Li, Z.; Wright, T.; Hooper, A.; Crippa, P.; Gonzalez, P.; Walters, R.; Elliott, J.; Ebmeier, S.; Hatton, E.; Parsons, B. Towards InSAR Everywhere, All the Time, with Sentinel-1. *Int. Arch. Photogramm. Remote Sens. Spat. Inf. Sci.* **2016**, *41*, 763–766. [CrossRef]

30. Hodson, T.O. Root Mean Square Error (RMSE) or Mean Absolute Error (MAE): When to Use Them or Not. *Geosci. Model Dev. Discuss.* **2022**, *15*, 5481–5487. [CrossRef]
31. Goldstein, R.M.; Werner, C.L. Radar Interferogram Filtering for Geophysical Applications. *Geophys. Res. Lett.* **1998**, *25*, 4035–4038. [CrossRef]
32. Rabus, B.; Eineder, M.; Roth, A.; Bamler, R. The Shuttle Radar Topography Mission—A New Class of Digital Elevation Models Acquired by Spaceborne Radar. *ISPRS J. Photogramm. Remote Sens.* **2003**, *57*, 241–262. [CrossRef]